Journal of Power Sources 188 (2009) 156–162

Contents lists available at ScienceDirect

Journal of Power Sources

journal homepage: www.elsevier.com/locate/jpowsour

A high performance composite ionic conducting electrolyte for intermediate temperature fuel cell and evidence for ternary ionic conduction

Chun Xia [a], Yi Li [b], Ye Tian [a], Qinghua Liu [a], Yicheng Zhao [a], Lijun Jia [a], Yongdan Li [a,*]

[a] Tianjin Key Laboratory of Applied Catalysis Science and Technology and State Key Laboratory for Chemical Engineering, School of Chemical Engineering, Tianjin University, Tianjin 300072, China
[b] Department of Chemistry, Tianjin University, Tianjin 300072, China

ARTICLE INFO

Article history:
Received 20 October 2008
Received in revised form
19 November 2008
Accepted 19 November 2008
Available online 27 November 2008

Keywords:
Doped ceria
Composite electrolyte
Intermediate temperature fuel cell
Ternary ionic conduction
Molten carbonate fuel cell

ABSTRACT

The performance of a composite electrolyte composed of a samarium doped ceria (SDC) and a ternary eutectic carbonate melt phase was examined. The formation temperature of a continuous carbonate melt phase is crucial to the high conductivity of this material. The electrolyte contains 30 and 50 wt% carbonate exhibited a sharp increase of conductivity at a temperature close to the melting point of the eutectic carbonate, *ca* 400 °C, which is more than 100 °C lower than those electrolytes using binary carbonate. At around 650 °C, and with CO_2/O_2 used as the cathode gas, the fuel cell gave a power output 720 mW cm^{-2} at a current density 1300 mA cm^{-2}. Water was measured in both the anode and cathode outlet gases and CO_2 was detected in the anode outlet gas. When discharged at 800 mA cm^{-2}, a stable discharge plateau was obtained. The CO_2 in the cathode gas enhances the power output and the stability of the single cell. Based on these experimental facts, a ternary ionic conducting scheme is proposed and discussed.

1. Introduction

High temperature fuel cells, e.g. solid oxide fuel cell (SOFC), have received much attention in recent years because of their high efficiency, high tolerance to impurities, and flexibility of fuels [1–3]. Conventional SOFC employs a ceramic oxide electrolyte, e.g. yttrium-stabilized zirconia, which requires a temperature as high as 800–1000 °C to achieve sufficient oxygen ion conductivity. However, such a high temperature poses a great challenge to the materials used in the fuel cell [4–6].

For operating at a low temperature, a high ionic conductivity of the electrolyte material is required. The improvement of zirconia, ceria and perovskite type oxide with various techniques has been a hot research topic [7–9]. Many new solid electrolytes have been explored [10–13]. Recently, salt–ceria-composite electrolyte material showed promising behavior [14–16]. The incorporation of molten inorganic salt into porous ceria-based oxide suppresses effectively the electronic conductivity and enhances the ionic conductivity, thus leads to an excellent cell performance at intermediate temperatures. These materials are found to be multi-ionic (O^{2-}/H^+) conductor with an overall ionic conductivity of around 0.1 S cm^{-1} at 600 °C [17]. A concept of binary ionic conduction was proposed to be superior to single ionic conduction in SOFCs [17,18]. It was assumed that when hydrogen and air are used as the fuel and the oxidant, the ceria bulk phase and the interface of the composite material provide the ionic conduction pathways for O^{2-} and H^+, respectively [18]. In literature, researchers focused on ceria–binary carbonate composite electrolyte, such as samarium doped ceria (SDC) with binary carbonate, e.g. SDC–Li/Na_2CO_3 and SDC–Li/K_2CO_3. However, a ternary carbonate Li/Na/K_2CO_3 has a further lower melting point [19], based on which it may compose a better electrolyte. In this work, SDC and Li/Na/K ternary carbonate salt was used to make up a composite electrolyte. A CO_2/O_2 gas mixture was used as the cathode gas and hydrogen as the anode gas. The performance of the fuel cell was investigated. A concept of ternary ionic conduction is proposed and discussed.

2. Experimental

2.1. Preparation of the composite electrolyte

SDC powder with a composition $Ce_{0.8}Sm_{0.2}O_{1.9}$ was prepared by an oxalate coprecipitation technique [20]. $Ce(NO_3)_3{\cdot}6H_2O$ and Sm_2O_3 were dissolved in diluted nitrate acid to form solutions containing 1 mol l^{-1} $Ce(NO_3)_3$ and $Sm(NO_3)_3$, respectively. Then the two solutions were mixed according to the prescribed ratio. Oxalate acid, 2 mol l^{-1}, was used as a precipitator to form the oxalate precursor. The precipitate was vacuum-filtrated and washed with

* Corresponding author. Tel.: +86 22 27405613; fax: +86 22 27405243.
E-mail address: ydli@tju.edu.cn (Y. Li).

0378-7753/$ – see front matter © 2008 Elsevier B.V. All rights reserved.
doi:10.1016/j.jpowsour.2008.11.068

Table 1
The composite electrolyte samples used in this work.

Composite name	Weight ratio SDC:$(Li/Na/K)_2CO_3$	Volume ratio SDC:$(Li/Na/K)_2CO_3$
SDC-10LNK	90:10	74.5:25.5
SDC-30LNK	70:30	43.1:56.9
SDC-50LNK	50:50	24.5:75.5

deionized water for three times. Then it was dispersed in ethanol by ultrasonic treatment. After another time of filtration, the material was dried at 100 °C overnight, followed by calcination at 650 °C for 2 h to obtain SDC powder. Li_2CO_3, Na_2CO_3, K_2CO_3 were mixed thoroughly with a mol ratio of 43.5:31.5:25, and heated at 600 °C in air for 1 h to form a ternary eutectic salt. The eutectic salt and SDC were mixed with various weight ratios, and then ground with an agate mortar. The material was calcined at different temperatures in air for 1 h. The compositions of the SDC–carbonate composite electrolyte (SCCE) are listed in Table 1. The volume ratio of each component is calculated from the density of the pure components at room temperature. The density of SDC is 7.12 g cm^{-3} which was calculated from the single cell data measured by XRD [21] and the density of the $(Li/Na/K)_2CO_3$ salt is 2.35 g cm^{-3}. The composite electrolyte powder was pressed at 300 MPa into a cylindrical pellet with a diameter of 13 mm and thickness of 1 mm using a uniaxial die-pressing technique. The green pellets were then sintered at 650 °C for 1 h. Silver electrodes were subsequently prepared by painting silver paste onto either sides of the pellet for conductivity test.

2.2. Characterization

The powder X-ray diffraction (XRD) patterns were recorded at room temperature using a D/max 2500 v/pc instrument (Rigaku Corp. Japan) with CuKα radiation, 40 kV and 200 mA power. The morphology of powders and the microstructure of sintered pellets were observed with a PHILIPS XL 30 scanning electron microscope (SEM). The phase transition behavior of the composite was measured by PerkinElmer Diamond TG/DTA in air with a heating rate of 4 °C min^{-1}. The electrical conductivity of the pellet was measured in air by a.c. impedance spectroscopy in a temperature range of 300–650 °C using an electrochemical workstation, CHI660B, made by Cheng Hua Corp in China, in a frequency range from 1 Hz to 100 kHz with a bias voltage of 5 mV.

2.3. Fuel cell test

A trilayer single cell structure was made by a co-pressing technique. The anode material was a mixture of NiO (50 vol.%) and the SCCE (50 vol.%). The cathode was made by mixing of SCCE (50 vol.%) and a lithiated NiO powder (50 vol.%) prepared by solid-state reaction of LiOH and NiO at 700 °C for 3 h [22]. The anode, electrolyte and cathode powders were fed into the die layer-by-layer and pressed into a cylindrical pellet at 300 MPa. The pellet was sintered at 650 °C for 1 h in air. The trilayer pellet has a size of 13 mm in diameter and 1.5 mm in thickness. The thickness of each layer was measured with an optical microscope. Silver paste was coated afterwards on each side to act as the current collector. A homemade setup was used for the performance measurement of the fuel cell assembly. The fuel cell was tested in a temperature range of 400–650 °C under atmospheric pressure. Hydrogen and CO_2/O_2 (1:1 in vol.%) gas mixtures were used as the fuel and oxidant, respectively. The gas flow rates in both sides were 100 ml min^{-1} (STP). The fuel cell *I–V* characteristics were measured by the SM-102 fuel cell tester made by San Mu Corp. China.

3. Results

3.1. Properties of the composite electrolyte

The powder XRD patterns of the ternary eutectic carbonate, pure SDC and SDC-30LNK SCCE sintered at various temperatures are presented in Fig. 1. The ternary carbonate shows complicated phase composition as Fig. 1 curve (a). Pure SDC has a single phase of cubic fluorite structure, which is in good agreement with JCPDS file 34-394. The average crystallite size of the SDC is 26 nm calculated from Scherrer formula $D = 0.9\lambda/\beta\cos\theta$, where λ is the wavelength of the X-ray, θ the diffraction angle. $\beta = (\beta_m^2 - \beta_s^2)$, β_m is the observed half height width of the (1 1 1) reflection, and β_s is that of a standard sample of CeO_2 [23]. For the composite sample sintered at 200 °C, the major phase is cubic fluorite but the carbonate phase shows a small peak at 29.5°. When the composite sample was sintered above 400 °C, the carbonate phase disappeared.

The SEM micrographs of the SCCEs with different carbonate contents are shown in Fig. 2. With this technique, the rough dimension of the grain size and the surface morphology can be observed. In SDC-10LNK, most of the crystallites have a rod like shape with aggregation forming attachments and twins between each others. In SDC-30LNK, some flat crystallites form. For SDC-50LNK, it shows a complete coverage of the SDC particle surface by the carbonate phase. Fig. 3(a–c) shows the surface morphologies of the SCCE pellets with different carbonate contents and sintered at 650 °C. From the images, it can be observed that as the salt content increases, the surface is covered more completely by the salt phase and the pellet becomes less porous. Fig. 3(d) presents a micrograph of the cross-section of SDC-30LNK pellet, the phase interface is clear and both the carbonate and the SDC form continuous phases.

The DTA curves of the SCCEs with different carbonate contents and that of the pure ternary carbonate are depicted in Fig. 4. Each curve has only one endothermic event attributed to the melt of the eutectic salt appeared in the temperature range of 300–500 °C. SDC-10LNK shows a very small peak in the temperature range of 350–400 °C with a peak temperature at 376 °C, which is much lower than the temperature ranges of the peaks for the other three samples. The increase of carbonate content leads to a slight shift of the peak temperature to higher range, locating at about 401, 402 and 403 °C for SDC-30LNK, SDC-50LNK and the ternary carbonate without SDC, respectively.

The conductivity versus temperature curves of the composite electrolyte with different carbonate ratios measured with the a.c.

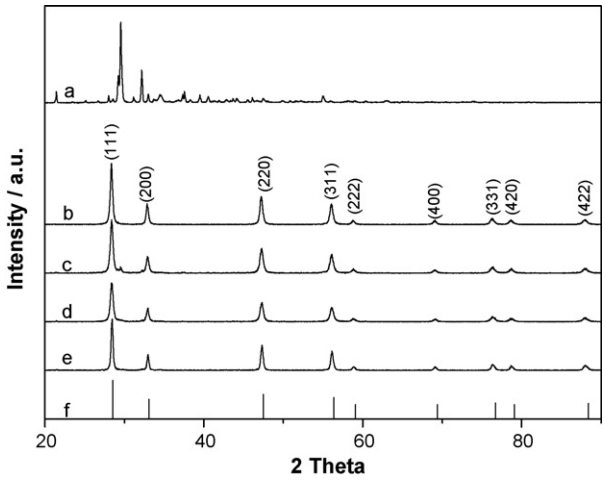

Fig. 1. XRD patterns. (a) $(Li/Na/K)_2CO_3$; (b) SDC; (c) SDC-30LNK sintered at 200 °C; (d) 400 °C; (e) 600 °C; (f) JCPDS file 34-394.

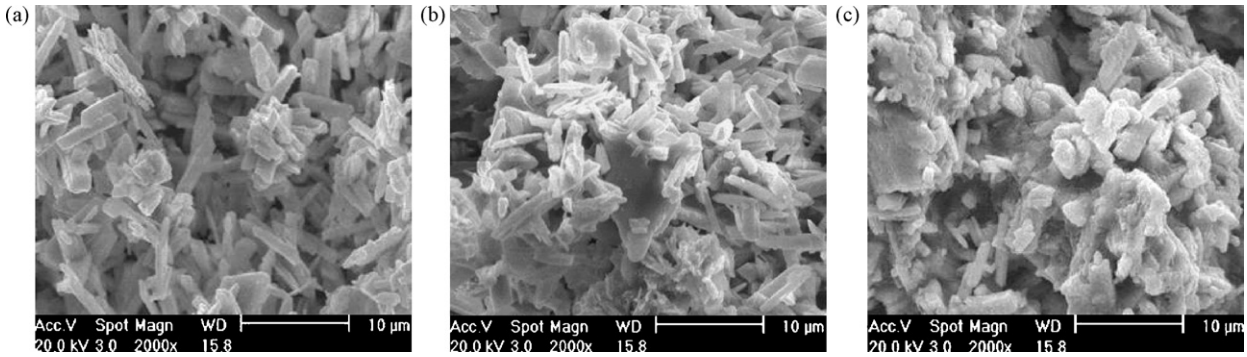

Fig. 2. SEM micrographs of composite electrolyte powder with different carbonate contents. (a) SDC-10LNK; (b) SDC-30LNK; (C) SDC-50LNK.

impedance technique are presented in Fig. 5. The conductivity of the composite electrolytes varies from 10^{-4} to 10^{-1} S cm^{-1} in the temperature range of 300–650 °C. The a.c. conductivity increases with the carbonate content and is much higher than that of the pure SDC in the temperature range above the melting point of the carbonate, *ca* 400 °C, especially for SDC-50LNK, which has a conductivity of two orders of magnitude higher than that of SDC. However, below this temperature, the conductivity decreases with the increase of the content of the carbonate. For the two samples with higher carbonate content, a sharp increase of the conductivity at a temperature closed to the melting point is observed.

3.2. Properties of the trilayer and performance of the single cell

I–V and *I–P* curves at 650 °C based on the composite electrolytes and with the mixed gas CO_2/O_2 used as the oxidant are illustrated in Fig. 6. In this case, the maximum output power densities of the single cells are 550, 720, 573 mW cm^{-2} for SDC-10LNK, SDC-30LNK, and SDC-50LNK used as the electrolytes, respectively. Fig. 7 gives the *I–V–P* characteristics of the single cell measured with SDC-30LNK electrolyte at different temperatures. The open-circuit voltages (OCV) are 1.11, 1.14, 1.06, 1.09 and 0.97 V at 650, 600, 550, 500, and 400 °C, respectively. The maximum output appeared at 650 °C and reached 720 mW cm^{-2} at a current density of 1300 mA cm^{-2}. Fig. 8 presents the discharge performance with time for the fuel cell measured with SDC-30LNK at 600 °C. The test is kept for 1 h. At the beginning of the discharge curve, a slight polarization is observed. The cell displays a constant output under a stable current density 800 mA cm^{-2} after 10 min for about 30 min, and then the voltage and power density improve slowly. Fig. 9 plots the curves showing the effect of the cathode oxidant gas. It shows reasonably that for the O_2/N_2 mixture the power density increases with the increase of the oxygen partial pressure. However, a remarkable improvement of fuel cell performance was observed over the

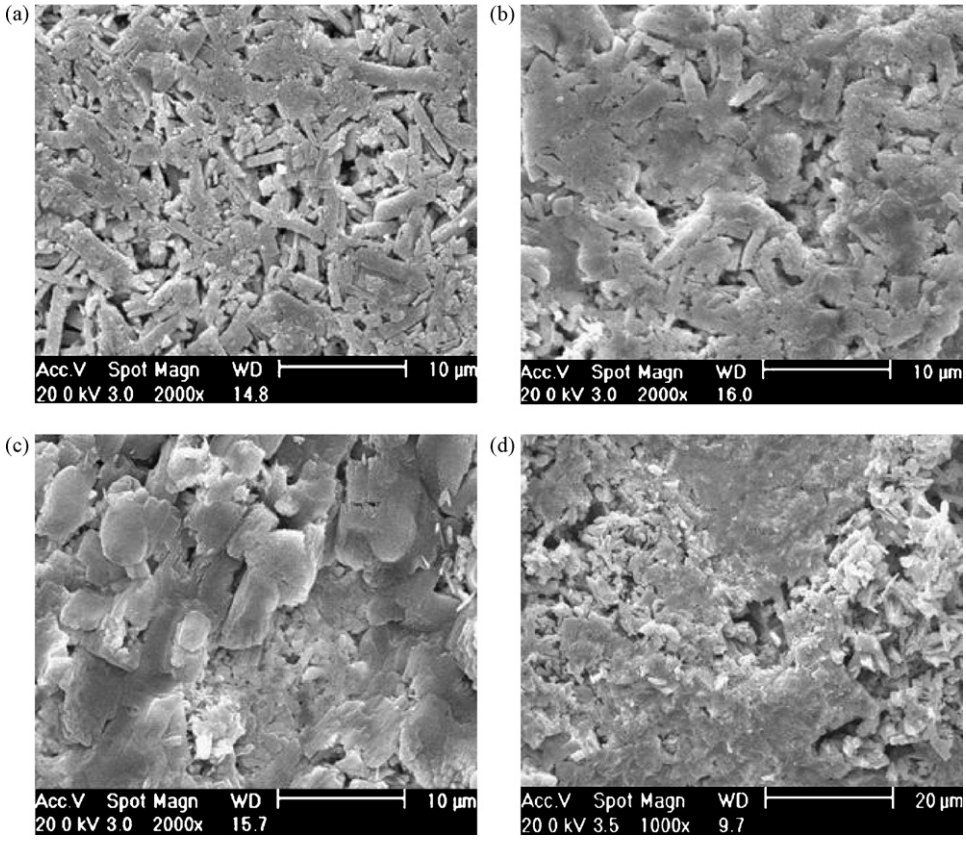

Fig. 3. SEM micrographs of composite electrolyte pellets. (a) SDC-10LNK; (b) SDC-30LNK; (c) SDC-50LNK; (d) the cross-section of SDC-30LNK.

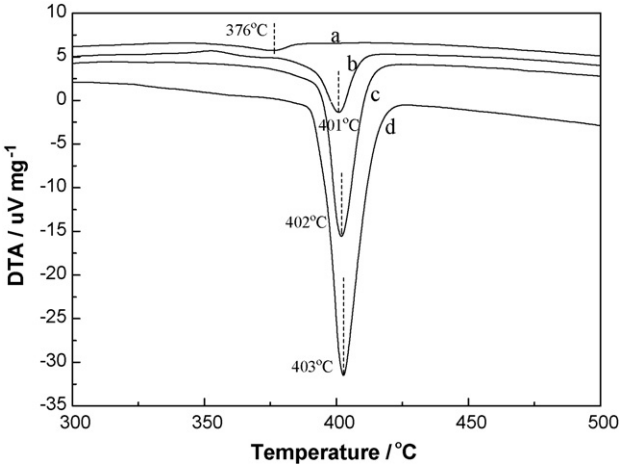

Fig. 4. DTA curves. (a) SDC-10LNK; (b) SDC-30LNK; (c) SDC-50LNK; (d) $(Li/Na/K)_2CO_3$.

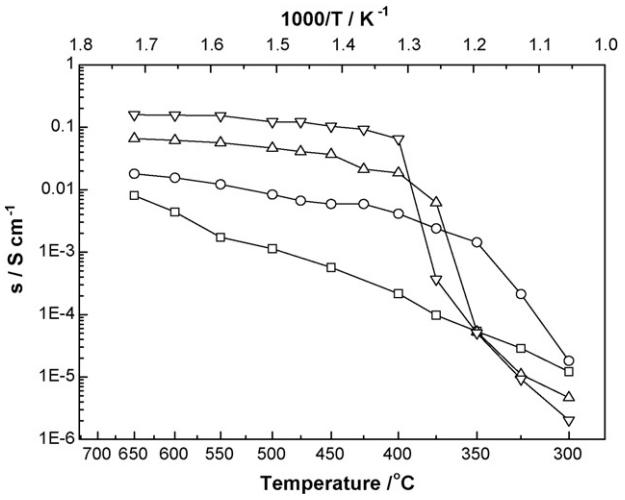

Fig. 5. Conductivity of different electrolytes at 300–650 °C. (□) SDC; (○) SDC-10LNK; (△) SDC-30LNK; (▽) SDC-50LNK.

O_2/N_2 mixture when the CO_2/O_2 mixture was used. It should be noted that, with CO_2/O_2 used, after the fuel cell was operated for 30 min, water was measured in the outlet gas of both sides and CO_2 was detected by GC in the anode outlet gas.

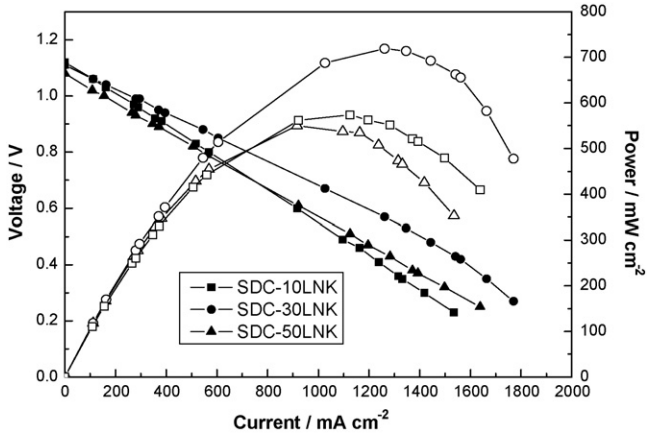

Fig. 6. Fuel cell performance with different composite electrolytes at 650 °C. (■, □) SDC-10LNK; (●, ○)SDC-30LNK; (▲, △)SDC-50LNK.

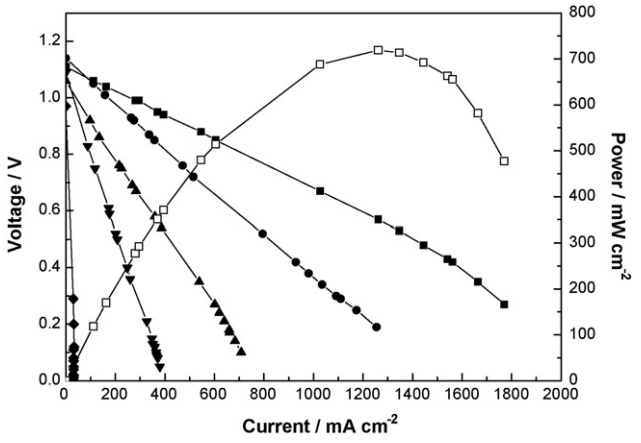

Fig. 7. *I–V* and *I–P* characteristics of the SDC-30LNK fuel cell in 400–650 °C. (■, □) 650 °C; (●) 600 °C; (▲) 550 °C; (▼) 500 °C; (♦) 400 °C.

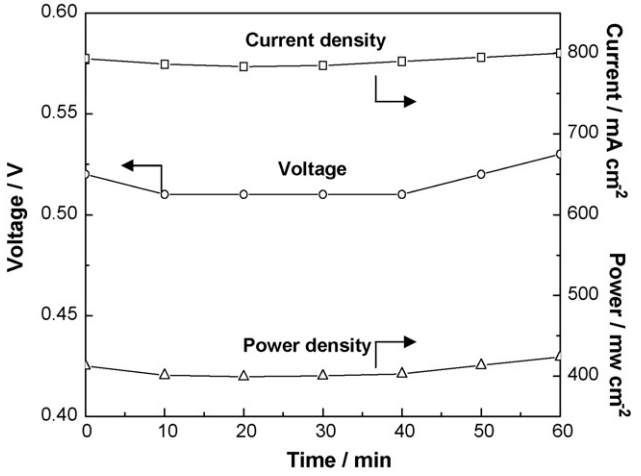

Fig. 8. Fuel cell performance curves with time for SDC-30LNK cell at 600 °C. (□) Current density; (○) voltage; (△) power density.

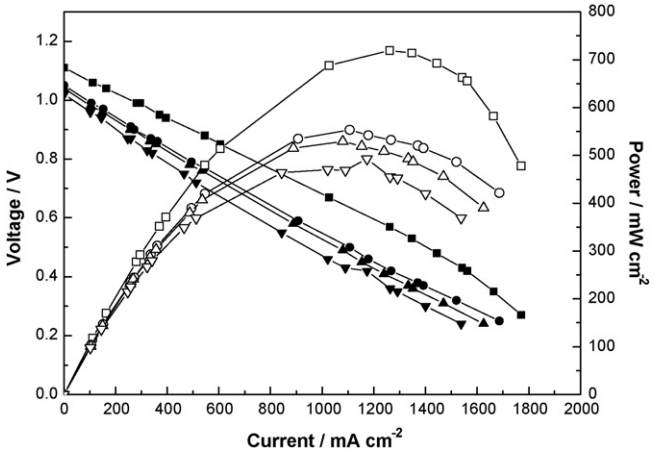

Fig. 9. The SDC-30LNK fuel cell performance at 650 °C with different cathode gases. (■, □) CO_2/O_2 (1:1), (●,○) O_2/N_2 (1:0), (▲,△) O_2/N_2 (1:1), (▼,▽) O_2/N_2 (1:4).

4. Discussion

4.1. The composite electrolyte

Jiang et al. [24] found that pure SDC has a fluorite structure and can be formed from the oxalate precursor above 350 °C.

Here, we reconfirm this result. According to the DTA curves, the ternary carbonate forms a eutectic salt and has a melting point from 376 to 403 °C depending on the ratio of the carbonate to the SDC. For SDC-30LNK, if sintered at 400 and 600 °C, the material shows an exactly same diffraction pattern as that of the pure SDC, indicating that the carbonates exist in an amorphous form. This was also reported by the other authors [25–27]. Here, the carbonates melted and coated on the SDC particles during the heat-treatment. Whether or not there is any reaction between the two phases, especially at the interface, should be verified with more specific techniques, however, some previous works assumed no reaction happened between SDC and molten carbonate [25].

From the SEM images, it can be seen that with the increase of the carbonate content, the surface of SDC is covered by carbonate more completely, and the carbonate phase becomes continuous when reach 30 wt%. Consequently, continuous phase interface is formed. Many pores can be seen on the surface of the SCCE in Fig. 3, which indicates that the electrolyte is not gas-tight at temperatures lower than the melting point of the carbonate phase. This lowers the OCV as shown in Fig. 7, OCV = 0.97 V at 400 °C. The porous structure indicates a poor chemical and mechanical affinity between the solid salt and oxide phases [25]. Above the melting point, the molten carbonate phase has a good wet ability to SDC surface and fills in the pores thus a gas-tight electrolyte forms. This is proved by the high OCV, >1.10 V, above the melting point. It should be noted that the OCV measured here is a bit higher than the standard OCV of a H_2/O_2 fuel cell. This is due to the presence of CO_2 in the cathode gas. As shown in Fig. 9, when O_2/N_2 was used as the cathode gas, the OCV was lower than that when CO_2/O_2 was used and was exactly the same as that of a H_2/O_2 fuel cell.

The a.c. conductivity of the SCCE varies from 10^{-4} to 10^{-1} S cm^{-1} in the temperature range of 300–650 °C, and the values of the SCCEs are 1–2 orders of magnitude higher than that of the pure SDC above the carbonate melting point. The SCCEs containing carbonate over 30 wt% exhibit a sharp increase of the conductivity at a temperature a bit lower than the melting point. This was explained by the appearance of a superionic conducting region, but here this phenomenon appeared more than 100 °C lower than literature results [28–30]. Maier [31] supposed that this region formed at the interface of the two conducting phases, where the cationic defect concentrations are much higher than that in the solid bulk. This phenomenon was enhanced due to the melting of the carbonate phase. Above this temperature, the transfer of ions (Li^+, Na^+, K^+, CO_3^{2-} and O^{2-} ions) from the constituent phases and the interface contributes to the conductivity. This is in consistent with the experimental result that higher carbonate content shows higher ionic conductivity. Below this temperature, the cationic defects near the interface are not activated and less mobile. In Fig. 5, it shows that the SCCEs with lower carbonate content have higher conductivity below the transition temperature than those with higher carbonate content. In this case, the O^{2-} conducting through the SDC bulk dominates, and the SDC phase is not very continuous because of the pores and the separation by a less conductive solid carbonate phase, so the O^{2-} conduction paths are insufficient [32]. The interfacial superionic conduction is enhanced when the carbonate phase melts, which is considered as an interfacial effect due to the formation of a high ion concentration with high mobility [33]. The melting point of the ternary carbonate used in this work, i.e. $(Li/Na/K)_2CO_3$, is more than 100 °C lower than the binary carbonate used in literature [32,34]. The superionic conduction can be formed at a lower temperature, which is the reason why the SCCE here has a higher conductivity compared to the literature results obtained with binary carbonates at temperatures below 500 °C.

4.2. Performance of single cell

When SDC-30LNK was used, the fuel cell gave the maximum output power density among the electrolyte samples examined. In this case, the volume ratio of SDC and carbonate was close to unity. Wu and Liu [35] found previously that the carbonate phase became continuous when its volume fraction is around 35%. In [18,32], it was assumed that oxygen ion and proton conductions happened in the SDC phase and along the interface, respectively. Therefore, when the carbonate formed a continous phase and dispersed uniformly on the SDC particle surface, consecutive interface was formed for proton conduction. This improved the fuel cell power output further.

In this work, when CO_2/O_2 mixed gas was employed as the oxidant, the OCV of the single cell is higher than that of a typical SDC electrolyte single cell, which seldom exceeds 0.96 V above 450 °C due to the electronic conduction of SDC resulting from the reduction of Ce^{4+} to Ce^{3+} in H_2 atmosphere [36,37]. In this work, the electronic conductivity of SDC was suppressed effectively by the introduction of enough amount of carbonate. The molten carbonate in the composite electrolyte formed a relatively dense electrolyte layer which helped also to avoid the gas crossover. The maximum power density achieved here is higher than that of the solid oxide fuel cells with a single-phase doped ceria electrolyte membrane and the conventional molten carbonate fuel cell (MCFC) operated at 650 °C [38–40]. This work proves that high-performance single cell with thick electrolyte (~0.5 mm) can be prepared by one-step pressing technique without a complicated film-preparation step.

When CO_2/O_2 gas mixture was used as the oxidant, as shown in Fig. 9, the fuel cell had a higher power density than that of when O_2/N_2 gas mixtures were used. Moreover, CO_2 was detected by GC in the anode outlet gas. It means that CO_3^{2-} conduction from cathode to anode happened in the composite electrolyte, which improves fuel cell performance further. Water was observed in the outlet gases of both sides. These facts indicate that the SCCE conducts H^+, O^{2-}, and CO_3^{2-} simultaneously.

4.3. Concept of ternary ionic conduction

It is plausible that in the composite electrolyte of this work, ternary ionic conduction, i.e. proton, oxygen and carbonate ions transfer simultaneously, happened. A scheme can be proposed as Fig. 10. When only O^{2-} ion conduction happens, the cell reactions are similar as in a SOFC, i.e. reactions (1–3) happens:

$$\text{Anode}: H_2 + O^{2-} \rightarrow H_2O + 2e \quad (1)$$

$$\text{Cathode}: (1/2)O_2 + 2e \rightarrow O^{2-} \quad (2)$$

$$\text{Overall reaction}: H_2 + (1/2)O_2 \rightarrow H_2O \quad (3)$$

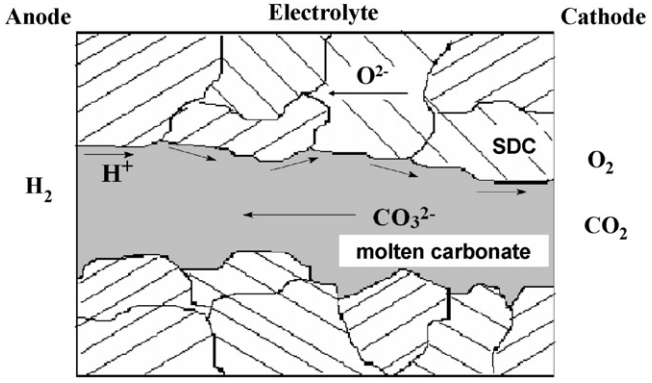

Fig. 10. Scheme of ternary ionic conduction process in the composite electrolyte.

O^{2-} conducts along the grain bulk and boundary of SDC as in the traditional solid oxide electrolyte.

In the case of CO_3^{2-} ion conduction, the cell reactions are similar as in a MCFC:

$$\text{Anode}: H_2 + CO_3^{2-} \rightarrow H_2O + CO_2 + 2e \quad (4)$$

$$\text{Cathode}: (1/2)O_2 + CO_2 + 2e \rightarrow CO_3^{2-} \quad (5)$$

$$\text{Overall reaction}: H_2 + (1/2)O_2 \rightarrow H_2O \quad (6)$$

CO_3^{2-} transfers through the bulk of molten carbonate as in a MCFC when CO_2/O_2 gas mixture is used as the cathode gas.

While in the case of only proton conducting exists, the cell reactions are written as in a proton exchange membrane fuel cell:

$$\text{Anode}: H_2 \rightarrow 2H^+ + 2e \quad (7)$$

$$\text{Cathode}: (1/2)O_2 + 2H^+ + 2e \rightarrow H_2O \quad (8)$$

$$\text{Overall reaction}: H_2 + (1/2)O_2 \rightarrow H_2O \quad (9)$$

H^+ is produced by hydrogen dissociation at the anode and may be absorbed by CO_3^{2-} to form a transitional state HCO_3^-, which may diffuse along the interface in the SDC side providing the possibility of proton transfer from anode to cathode near the interface [26]. The rationality of the interfacial conduction was also agreed by other authors [41]. However, HCO_3^- may also diffuse in the bulk carbonate phase.

In the previous works of fuel cells with H^+/O^{2-} bi-ionic conducting electrolytes, proton and oxygen ions conductions predominate, and the contribution of CO_3^{2-} ion transfer in the molten carbonate bulk phase is neglected, because no CO_3^{2-} was supplied, i.e. no CO_2 in the oxidant gas [42]. Here, O_2/CO_2 gas mixture was used as the cathode gas, which provides CO_3^{2-} ion and stimulates CO_3^{2-} ion conduction in the molten carbonate bulk phase [43]. This was confirmed by the detection of CO_2 in the anode outlet gas. Fig. 9 illustrates the superiority of the ternary ionic conduction to binary ionic conduction.

In a traditional MCFC, the electrolyte is a molten carbonate retained in a porous $LiAlO_2$, which is an insulator. In order to achieve sufficient conductivity, the electrolyte contains 60–70 vol.% molten carbonate, and the fuel cell is operated at around 650 °C. The ionic transport is governed by CO_3^{2-} ion conduction [44]. The typical power output of a MCFC is 150–250 mW cm^{-2} [45]. However, when SCCE is used, SDC functions not only as a support, but also as an O^{2-} conductor and a supplier of a fast O^{2-}/H^+ conduction path [16]. Moreover, the existence of proton conduction promotes the electrode reaction and the transport between the electrolyte and the electrode [16]. However, the comparative importance of proton transportation along the interface and in the carbonate phase needs to be verified with more specific techniques. Quantitative measurement of the electrode kinetics and on-*oprendo* characterization of the ion transportations are helpful to validate the mechanism proposed here.

5. Conclusions

A composite material based on SDC and $(Li/Na/K)_2CO_3$ ternary mixed eutectic salt was developed and used as the electrolyte of an intermediate temperature fuel cell. This material has a much higher ionic conductivity than pure SDC in the temperature range above 400 °C, which is close to the melting point of the carbonate phase in the composite. Further characterization reveals that the melting of carbonate is a key factor for the good performance of this material. Below the melting point, the conductivity decreases with the increase of the carbonate content, indicating that the solid carbonate phase is not a good ionic conductor. The OCV goes up effectively after the melting, which means that before melting the material is porous and not gas-tight. The molten carbonate fills the pores and has a good wet ability with the SDC surface. The XRD results indicate that the carbonates exist in an amorphous form.

When this material was used to make up a fuel cell and CO_2/O_2 gas mixture was used as the cathode oxidant gas, the cell exhibited a good performance with a peak power output 720 mW cm^{-2} at a current density of 1300 mA cm^{-2} at 650 °C. The experimental facts indicate that ternary $O^{2-}/H^+/CO_3^{2-}$ conduction happened in the composite electrolyte, simultaneously. It assumes that O^{2-} and CO_3^{2-} conduct in the SDC and molten carbonate phases, respectively. H^+ may transfer along the interface and may be absorbed by CO_3^{2-} to form a transitional state HCO_3^-, which transfers in the carbonate side. The fuel cell based on the ternary ionic conducting material shows good performance and stability in intermediate temperature range.

Acknowledgements

This work has been supported by the Natural Science Foundation of China under contract numbers 20425619 and 20736007. The work has been also supported by the Program of Introducing Talents to the University Disciplines under file number B06006, and the Program for Changjiang Scholars and Innovative Research Teams in Universities under file number IRT 0641.

References

[1] K.V. Kordesh, G.R. Simader, Chem. Rev. 95 (1995) 191–207.
[2] B. Zhu, J. New Mater. Electrochem. Syst. 4 (2001) 239–251.
[3] K. Joon, J. Power Sources 71 (1998) 12–18.
[4] J.W. Fergus, J. Power Sources 162 (2006) 30–40.
[5] B. Zhu, J. Energy Res. 30 (2006) 895–903.
[6] B.C.H. Steele, A. Heinzel, Nature 414 (2001) 345–352.
[7] Z.G. Lv, P. Yao, R.S. Guo, F.Y. Dai, Mater. Sci. Eng. A 458 (2007) 355–360.
[8] B.C.H. Steele, Solid State Ionics 129 (2000) 95–110.
[9] T. Ishihara, H. Matsuda, Y. Takita, J. Am. Chem. Soc. 116 (1994) 3801–3803.
[10] B. Bastide, R. Enjalbert, P. Salles, J. Galy, Solid State Ionics 158 (2003) 351–358.
[11] D.M. López, J.P. Martínez, Solid State Ionics 178 (2007) 1366–1378.
[12] D. Prakash, T. Delahaye, O. Joubert, M.T. Caldes, Y. Piffard, J. Power Sources 167 (2007) 111–117.
[13] B. Zhu, Z.G. Luo, C.R. Xia, Mater. Res. Bull. 34 (1999) 1507–1512.
[14] B. Zhu, X.R. Liu, P. Zhou, J. Mater. Sci. Lett. 20 (2001) 591–594.
[15] B. Zhu, J. Power Sources 93 (2001) 82–86.
[16] B. Zhu, X.C. Liu, P. Zhou, X.T. Yang, Z.G. Zhu, W. Zhu, Electrochem. Commun. 3 (2001) 566–571.
[17] B. Zhu, J. Power Sources 114 (2003) 1–9.
[18] B. Zhu, X.T. Yang, J. Xu, Z.G. Zhu, S.J. Ji, M.T. Sun, J.C. Sun, J. Power Sources 118 (2003) 47–53.
[19] J.R. Selman, H.C. Maru, in G. Mamantov, J. Braunstein, Advances in Molten Salt Chemistry, vol. 4, Plenum Press, New York and London, 1981, pp.159–389.
[20] R.S. Torrens, N.M. Sammes, G.A. Tompsett, Solid State Ionics 111 (1998) 9–15.
[21] Y.F. Gu, G. Li, G.Y. Meng, Mater. Res. Bull. 35 (2000) 297–304.
[22] J.B. Huang, L.Z. Yang, R.F. Gao, Z.Q. Mao, C. Wang, Electrochem. Commun. 8 (2006) 785–789.
[23] K. Singh, S.A. Acharya, S.S. Bhoga, Ionics 13 (2007) 429–434.
[24] C.R. Jiang, J.J. Ma, X.Q. Liu, G.Y. Meng, J. Power Sources 165 (2007) 134–137.
[25] Q.X. Fu, S.W. Zha, W. Zhang, D.K. Peng, G.Y. Meng, B. Zhu, J. Power Sources 104 (2002) 73–78.
[26] J.B. Huang, Z.Q. Mao, L.Z. Yang, R.R. Peng, Eelectrochem. Solid State 8 (9) (2005) A427–A440.
[27] X.D. Wang, Y. Ma, R. Raza, M. Muhammedb, B. Zhu, Electrochem. Commun. 10 (2008) 1617–1620.
[28] A. Bodén, J. Di, C. Lagergren, G. Lindbergh, C.Y. Wang, J. Power Sources 172 (2007) 520–529.
[29] W. Zhu, C.R. Xia, D. Ding, X.Y. Shi, G.Y. Meng, Mater. Res. Bull. 41 (2006) 2057–2064.
[30] B. Zhu, S. Li, B.E. Mellander, Electrochem. Commun. 10 (2008) 302–305.
[31] J. Maier, Prog. Solid State Chem. 23 (1995) 171–263.
[32] J.B. Huang, Z.Q. Mao, Z.X. Liu, C. Wang, Electrochem. Commun. 9 (2007) 2601–2605.
[33] B. Zhu, X.R. Liu, Z.G. Zhu, R. Ljungberg, Int. J. Hydrogen Energ. 33 (2008) 3385–3392.
[34] J.B. Huang, Z.Q. Mao, Z.X. Liu, C. Wang, J. Power Sources 175 (2008) 238–243.
[35] Z.L. Wu, M.L. Liu, Solid State Ionics 93 (1997) 65–84.
[36] H. Inaba, H. Tagawa, Solid State Ionics 83 (1996) 1–16.
[37] X.G. Zhang, M. Robertson, C. Deĉes-Petit, W. Qu, O. Kesler, R. Maric, D. Ghosh, J. Power Sources 164 (2007) 668–677.
[38] S. Piñol, M. Morales, F. Espiell, J. Power Sources 169 (2007) 2–8.

[39] M. Enoki, J.W. Yan, H. Matsumoto, T. Ishihara, Solid State Ionics 177 (2006) 2053–2057.
[40] S.D. Kim, S.H. Hyun, J. Moon, J.H. Kim, R.H. Song, J. Power Sources 139 (2005) 67–72.
[41] B. Zhu, I. Albinsson, C. Andersson, K. Borsand, M. Nilsson, B.-E. Mellander, Electrochem. Commun. 8 (2006) 495–498.
[42] S. Li, X.D. Wang, B. Zhu, Electrochem. Commun. 9 (2007) 2863–2866.
[43] Q.H. Liu, Y. Tian, C. Xia, L.T. Thompson, B. Liang, Y.D. Li, J. Power Sources 185 (2008) 1022–1029.
[44] G.Y. Meng, Q.X. Fu, S.W. Zha, C.R. Xia, X.Q. Liu, D.K. Peng, Solid State Ionics 148 (2002) 533–537.
[45] J.R. Selman, J. Power Sources 160 (2006) 852–857.